The Role of Inhibition in an Associative Memory Model of the Olfactory Bulb

Ofer Hendin and David Horn

School of Physics and Astronomy
Raymond and Beverly Sackler Faculty of Exact Sciences
Tel-Aviv University, Tel-Aviv 69978, Israel
hendin@neuron.tau.ac.il horn@vm.tau.ac.il

Misha V. Tsodyks

Neurobiology Dept.
Brain Research Building - Weizmann Institute
Rehovot 76100 Israel
bnmisha@wicc.weizmann.ac.il

Abstract

The external plexiform layer is where the interactions between the mitral (excitatory) and granule (inhibitory) cells of the olfactory bulb (OB) take place. Two outstanding features of these interactions are that they are dendrodendritic, and that there seem to be none between excitatory cells. The latter are the ones that are usually accreditted with the role of forming Hebbian cell assemblies. Hence it would seem that this structure lacks the necessary ingredients for an associative memory system.

In this paper we show that in spite of these two properties this system can serve as an associative memory. Our model incorporates the essential anatomical characteristics of the OB. The memories in our system, defined by Hebbian mitral assemblies, are activated via the interactions with the inhibitory granule cells. The nonlinearity is introduced in our model via a sigmoid function that describes neurotransmitter release in reciprocal dendrodendritic synapses. The capacity (maximal number of odors that can be memorized) depends on the sparseness of coding which is being used. For very low memory activities, the capacity grows as a fractional power of the number of neurons. We validate the theoretical results by numerical simulations.

An interesting result of our model is that its capacity increases as a function of the ratio of inhibitory to excitatory populations. This

may provide an explanation for the dominance of inhibitory cells in the olfactory bulb.

1 Introduction

The neuronal anatomy of the olfactory bulb (OB) was investigated in great detail, yet its function is an open problem (2). In the last decade, numerous experiments, e.g. (25), have indicated that activation of the bulb is modified with learning experience. In these experiments, recordings of EEG signals from the surface of the rabbit's olfactory bulb were shown to change during the first few successive applications of an odor. It was only after a learning period that the EEG displayed consistent patterns of activation which were repeated on applications of an odor. In recent studies (16), it was found that in insects[1] odors evoked specific activation of coherently firing oscillating neural assemblies. These authors also observed that different odors evoked activity of specific and overlapping ensembles of neurons that can be considered as attractors of the dynamics.

Sensory information enters the bulb via the olfactory nerve which converges onto the glomeruli structures. In the glomeruli, axons of sensory cells terminate on the distal dendrites of excitatory mitral/tufted[2] cells which in turn project their output onto the olfactory cortex and other processing centers. In the *external plexiform layer* (EPL) of the bulb, located between the glomeruli and the somas of the mitral cells, some form of information processing takes place via interactions between the dendrites of the mitral cells and those of inhibitory granule cells. [3] The olfactory granular cells are small neurons with cell bodies that are located proximal to mitral cell bodies and have dendrites extending into the external plexiform layer. The interactions between the two cell types are dendrodendritic in nature, and are mainly mediated via reciprocal[4] synaptic connections (over 80%).

It is usually believed that the piriform cortex (mushroom bodies) is the

[1]The architecture of the olfactory nervous system of insects shows many fundamental similarities to that of vertebrates.

[2]Henceforth we shall refer to mitral cells only, since mitral and tufted cells are similar in their behavior and function.

[3]The ratio of granule to mitral cell populations is estimated (21) to be 50:1.

[4]A reciprocal synapse is the arrangement of presynaptic dendrites, interacting so that a mitral cell can excite the granule cell and the granule cell can inhibit the mitral cell.

location of olfactory memory (8)(9). The OB is assumed to have some computational role in cleaning up the signal that arrives at the cortex. This involves both overcoming noise and handling the problem of the rapid turnover in the sensory cells (4)(18). In this paper we investigate whether, in fact, the EPL region of the olfactory bulb can serve as an Attractor Neural Network (ANN). The biological motivation is twofold. The first is that an ANN can account for the improving of signal quality. Although there is evidence for convergence of the distributed sensory cells to well defined and distinct subsets of glomeruli (27)(19), the exact connectivity of a newborn sensory cell to a mitral cell in a glomerulus cannot be assumed to be that of the dead cell it replaces. This is where an ANN can come in handy. Attractor dynamics can serve as a mechanism for correcting the intrinsic instability of odor signals. The second motivation is that the bulb projects directly to several other brain structures. Hence it would seem advantageous if it had memory capabilities.

There are two major differences between the interactions of the mitral and granular neurons, as observed in the EPL, and conventional associative memory models. The first is that there is no direct evidence for excitatory-excitatory interactions, that are usually assumed to be the basis for formation of Hebbian cell assemblies. The second is that most interactions are dendrodendritic (21)(15) in contradistinction to the axodendritic interactions that are the rule in the cortex. Hence this system lacks the nonlinearity involved in generating the action potential in the axon that is an important ingredient in ANN models.

In our model, as described in section 2, we introduce nonlinearity through a sigmoid structure in the reciprocal dendrodendritic synapses. Since generation of action potentials in the dendrites of both cell types is rare (21)(28), we relate the activity in a reciprocal synapse to voltage changes. The sigmoid describes a saturating probabilistic process of neurotransmitter release. We show that relying on inhibition and disinhibition we can construct an ANN even in the absence of excitatory-excitatory connections. The resulting model can be compared to other attractor neural networks with low activity levels, such as those discussed by Willshaw et al. (30) and Tsodyks & Feigelman (26). We explore the conditions under which the large inhibitory population increases the network's capability of storing memory patterns of sparse activity.

The next section is dedicated to the mathematical formulation of our model. In section 3 we discuss its capacity and validate the results with simulations in section 4. In section 5 we investigate a model based on generalized Hebbian learning, in which we allow for different sizes of inhibitory and excitatory cell populations. We explain the advantage of larger inhibitory populations, and demonstrate the satisfactory performance of the model with numerical simulations.

2 Mathematical Formulation

We consider a system of N_m mitral and N_g granule cells. We introduce variables which denote release of neurotransmitter at reciprocal synapses. The probabilistic process governing the rate of neurotransmitter release is assumed to have the same general dependence on membrane potential as do spike rates. Denoting by M (G) the rate of neurotransmitter release from a mitral (granule) cell of membrane potential m (g), we write the dynamical equations:

$$M_i = \sigma(m_i) \quad \text{with} \quad \frac{dm_i}{dt} = -\frac{m_i}{\tau_m} - \sum_j J_{ij} G_j + I_i(t) + I_0 \tag{1}$$

$$G_i = \sigma(g_i) \quad \text{with} \quad \frac{dg_i}{dt} = -\frac{g_i}{\tau_g} + \sum_j W_{ij} M_j - \sum_j K_{ij} G_j \tag{2}$$

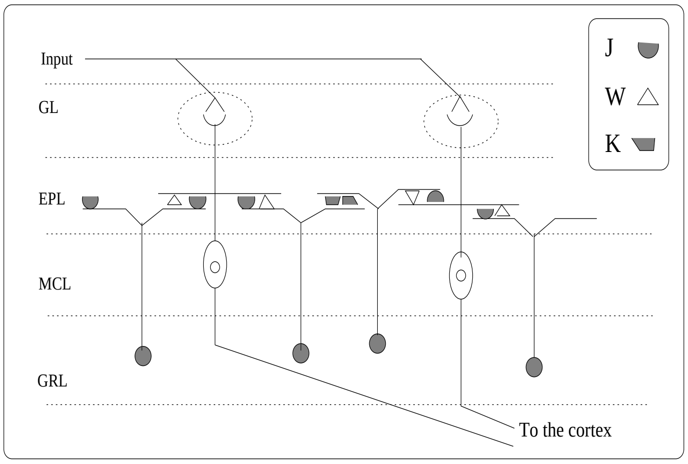

Figure 1: Schematic illustration of the network's architecture. Inhibitory neurons and their connections are denoted by gray color. GL, glomerular layer; EPL, external plexiform layer; MCL, mitral cell layer; GRL granule cell layer.

These equations describe interactions in the external plexiform layer, which is traversed by the proximal dendrites of mitral cells. The different neurons are coupled by the matrices J K, and W. All of the cell input and the effect of dendrodendritic (reciprocal) interactions at distal sites of mitral cells are denoted by the dendritic currents $I_i(t)$ and I_0. I_i represent specific inputs to different mitral cells which we will not need in our following analysis, where we will test the system using the conventional paradigm of an ANN which converges to a fixed point from some initial condition (13). However, because there are no excitatory interactions in our system, we have to employ a constant excitatory input, I_0, which may relate to the spontaneous background activity[5].

We make two assumptions regarding the behavior of granule cells. First, we assume that $\tau_g \ll \tau_m$. In this case, changes in G are rapid compared to changes in M. The second assumption is that the membrane potentials normally assume values such that the sigmoid function is in the linear regime. This is best described by the *limited linear threshold* approximation $G_i = \mathcal{L}\left(g_i\right)$, which vanishes for negative arguments, equals βg for positive ones with a cutoff at G_{max}.

$$\mathcal{L}(g) = \begin{cases} \beta\tilde{g} & g > \tilde{g} \\ \beta g & 0 < g \le \tilde{g} \\ 0 & g \le 0 \end{cases} \tag{3}$$

For the mitral cells we assume higher membrane potentials and, therefore, we approximate their sigmoid behavior by a step function $M_i = \Theta(m_i)$.

The equations of motion have fixed point solutions which allow for their interpretation as an ANN system. The fixed points can be described by:

$$M_i = \Theta\left(-\sum_j J_{ij} G_j + I_0\right) \tag{4}$$

$$G_i = \tau_g \mathcal{L}\left(\sum_j W_{ij} M_j - \sum_j K_{ij} G_j\right) \tag{5}$$

In this framework M_i have binary values, either 0 or 1, and G_i are continuous variables with an upper bound chosen as $\tau_g\beta\tilde{g} = 1$. We use the mitral

[5]The background activity in the olfactory bulb is discussed in detail in (25)

cells for the definition of memory states ξ_i^μ which we want to store and retrieve in this system. This is a natural choice, because mitral cells are the source of axonal projections to the cortex. The spike rates of mitral cells, as seen by the cortex, may be approximated by M_i, since they too are sigmoidal functions of the membrane potential m_i.

We define p binary memory patterns ξ^μ $(\mu = 1 \cdots p)$ of the form $M_i = \xi_i^\mu$. These patterns are fixed points of the dynamics specified above, and are stored in the network, using random choices of:

$$\xi_i^\mu = \begin{cases} 1 & \text{with prob. f} \\ 0 & \text{with prob. } 1 - f \end{cases} \tag{6}$$

Starting from a distorted pattern, the successful recall of a memory is the convergence of M_i to the correct pattern of activity, which forms a fixed point of the system (4,5). In fact, it is only a part of the fixed point structure, which should associate every ξ^μ with an η^μ which corresponds to the (hidden) representation of the granular layer $G_i = \eta_i^\mu$. The latter is a continuous representation, corresponding to the result of Eq. 5 for the input of $M = \xi^\mu$. For the consistency of the system, $M = \xi^\mu$ should also be the solution of Eq. 4 for the input $G = \eta^\mu$.

Let us now concentrate on equation 4. It depends on the matrix J of inhibitory synaptic connections. We propose to construct it via inhibitory-Hebbian learning. This rule implies that the strength of an inhibitory synapse is increased if activity of a presynaptic neuron coincides with the *absence* of activity on the postsynaptic site. For the given set of memories described above this can be implemented by

$$J_{ij} = \frac{1}{N_g} \sum_\mu (1 - \xi_i^\mu) \eta_j^\mu \tag{7}$$

In the following section we will discuss the stability of equation 4 under these conditions.

3 Signal to Noise Analysis

In order to analyze the behavior of the model, one has to calculate the inhibitory input to the mitral layer after presentation of one of the patterns, e.g. ξ^ν. From Eq. 4, this input field is given by:

$$\begin{aligned} h_i &= -\sum_{j=1}^{N_g} J_{ij}\eta_j^\nu \\ &= -\frac{1}{N_g}\sum_{\mu j}(1-\xi_i^\mu)\eta_j^\mu\eta_j^\nu = -S_i - R_i \end{aligned} \tag{8}$$

We have separated the sum in Eq. 8 into two contributions: The 'signal' S_i, which corresponds to the term with $\mu = \nu$,

$$S_i = \frac{1}{N_g}(1-\xi_i^\nu)\sum_j(\eta_j^\nu)^2, \tag{9}$$

and the 'noise' originating from all the other terms in Eq. 8:

$$R_i = \frac{1}{N_g}\sum_{j,\mu\neq\nu}(1-\xi_i^\mu)\eta_j^\mu\eta_j^\nu. \tag{10}$$

We are now in a position to state the conditions under which Eq. 4 can be satisfied. For the terms $\xi_i^\nu = 1$, for which the argument of the step function has to be positive, S_i vanishes and the only condition is that I_0 be bigger than the value of the noise term R_i. For the terms $\xi_i^\nu = 0$, for which M_i should vanish, S_i has a finite value, $S_i = \langle\eta^2\rangle$, which should be larger than $I_0 - R_i$.

To analyze the meaning of these conditions we assume that η_i^μ have a probability q of being non-zero, in which case they are describable by randomly continuous variables with an average value a. R_i has then an average value of $r = p(1-f)\langle\eta\rangle^2 = p(1-f)q^2a^2$ and fluctuates with standard deviation ρ given by:

$$\rho^2 = pf\langle\eta\rangle^4 + \frac{p^2}{N_g}\langle\eta\rangle^2\left(\langle\eta^2\rangle - \langle\eta\rangle^2\right) + \frac{p}{N_g}\langle\eta^2\rangle^2. \tag{11}$$

Both r and ρ increase with the number of patterns p. This means, first of all, that I_0 should also increase proportionally to the number of learned memories. Such a behavior may be invoked by requiring that feedback connections from the piriform cortex to the olfactory bulb will carry common excitation that is proportional to the general activity of the mitral cells. We will assume henceforth that I_0 carries this information. In simulations we choose it to be around $I_0 \approx 0.9\langle h\rangle$. Once such an assumption is made, no further limitation arises from the average noise. The standard deviation leads, however, to an upper limit on the possible number of patterns. It follows, that the maximal number of patterns, p_c, which can be successfully retrieved by the network is subject to the condition is that the noise amplitude will be small compared to the signal: $\rho/\langle\eta^2\rangle \ll 1$. To simplify the following discussion, we restrict our analysis to the case where the fraction of active neurons is small in both mitral and granule layers:

$$f \ll 1, \qquad \text{and} \qquad q \approx \frac{\langle\eta\rangle^2}{\langle\eta^2\rangle} \ll 1 \tag{12}$$

The parameter q is the fraction[6] of active granule cells, whose typical transmitter release rate is denoted by a. It can be shown that the condition (Eq. 12) on sparseness of the activity is a necessary condition for the network to be able to store many patterns, similar to the models of Willshaw (30) and Tsodyks & Feigelman (26). Different terms in the noise amplitude (Eq. 11) determine (for $N_g \to \infty$) the upper limit on the network's capacity. If q remains small but finite, the system is capable of storing a finite number of patterns:

$$p_c \approx \frac{1}{fq^2} \tag{13}$$

However, if q scales with the size of the inhibitory population so that $q < 1/(f^2 N_g)^{\frac{1}{3}}$, the second term in Eq. 11 becomes dominant, leading to:

$$p_c \approx \sqrt{\frac{N_g}{q}}. \tag{14}$$

Note that in both cases the capacity of the network is a decreasing function of the sparseness parameter q, which is controlled by the strength of the inhibitory intergranule interactions K, as will be discussed in the next section. When q is low, we learn that the capacity grows with the size of the granule layer N_g, which may be an indication of why there are so many more granule cells than mitral cells.

[6]The condition 12 is often referred to as a sparse coding of external stimuli.

We next consider two particular models in which the interactions, given by the matrices W and K, are specified, and analyze their role in the associative network.

4 Model I: Fixed Connections

We first consider a simple model, in which the interactions W and K are fixed. This will be later compared with a model in which Hebbian and inhibitory-Hebbian rules will be employed. Here we assume the connectivity between granule cells to be uniform,

$$K_{ij} = \frac{\kappa}{N_g}(1 - \delta_{ij}) \tag{15}$$

and choose a random connectivity matrix W. With this choice, all of the assumptions of the previous analysis are satisfied.

The assumption of uniform structure in the K matrix is done for convenience of computation. Taken literally it implies long-range connectivity between granule cells, which is not realistic. It can be shown, however, that strong inhibition among short range granule cells leads to the same result. Our analysis is based only on the average effect felt by each neuron.

The excitatory input to the granule cells upon the presentation of the pattern is (see Eqs. 5)

$$h_i^{ex} = \sum_j W_{ij}\xi_j^\mu. \tag{16}$$

This is a sum of large number (N_m) of random uncorrelated variables, and thus becomes a gaussian random field. Its average and variance are given by:

$$\begin{aligned} \langle h^{ex} \rangle &= f\langle W \rangle \\ v^2 = \mathrm{var}(h^{ex}) &= \frac{1}{N_m} f \mathrm{var}(W) \end{aligned} \tag{17}$$

where $\langle W \rangle$ and $\mathrm{var}(W)$ are moments of the random matrix elements of the rescaled interaction $N_m W_{ij}$. Note that the variance decreases with the size of the excitatory population. The second component of input to granule cells, originating from the feedback inhibition from other granule cells, is uniform over the whole population due to the uniformity of the matrix K:

$$h_i^{in} = -\sum_j K_{ij} G_j = -\kappa \langle \eta \rangle \qquad \text{for each } i \tag{18}$$

Here we used the fact that presenting the pattern ξ^μ to the mitral layer evokes the activity pattern η^μ which is given by the solution of Eq. 5. These patterns are uncorrelated for different μ due to the randomness of ξ^μ and W.

The distribution of activities (η) of the granule cells consists of a peak at zero, corresponding to the cells which are quiescent due to inhibition, and a gaussian tail of the remaining *active* neurons with average activity a. The fraction of cells in the tail, q, is a decreasing function of the strength of feedback inhibition (governed by κ). Quantitative analysis, outlined in the Appendix, gives the following asymptotic behavior in the limit of very strong inhibition:

$$\begin{aligned} \langle \eta \rangle &\approx v \frac{\sqrt{2log(\kappa)}}{\kappa} \\ q &\approx \frac{2log(\kappa)}{\kappa} \\ a \approx \frac{\langle \eta \rangle}{q} &= \frac{v}{\sqrt{2log(\kappa)}}. \end{aligned} \tag{19}$$

These results indicate that strong inhibition guarantees small fraction of active granule cells q. It also indicates that a penalty, in the form of small average transmitter release a, follows from strong inhibition. Its effects will be discussed in section 6.

4.1 Simulations

We simulated Model I using $N_m = 300$ neurons and verified the validity of our estimates. Each of the stored patterns was distorted (by approximately 5%), and the network was allowed to converge to its steady state. Calculating the overlap of the final state with the input, and averaging over all stored patterns, we plot the result in figure 2 versus $p/\sqrt{N_g}$. The observed scaling indicates that the analytic results (see Eq. 14) describe correctly the behavior of the network.

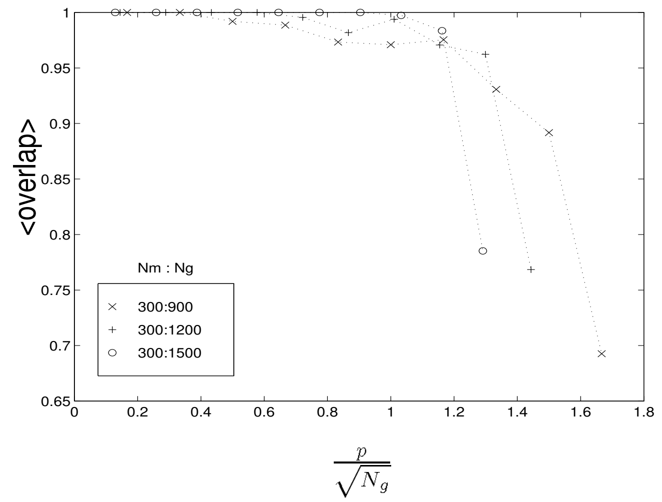

Figure 2: The average overlap of the system vs. $p/\sqrt{N_g}$. One can see how the curves pack together, indicating that this is the correct scaling variable. The points on the graph correspond to average results, obtained from 5 to 10 runs of the system, starting from an up to 5% distorted pattern that was picked randomly (with $f = 0.05$) from the pool of stored patterns.

Intuitively one may expect the capacity to increase with N_g because of the increase in the number of synapses. To see how it comes about we compare in Figure 3 networks with different N_g and observe the improvement in the signal to noise ratio due to such increase in the number of inhibitory cells. We compare here two networks with the same number of mitral cells in which we try to encode the same number of patters. It turns out that the network with the lower number of granule cells is above its critical capacity: the shown pattern is not reproduced consistently. The larger network performs well.

Despite the seemingly good performance demonstrated above, the simple model considered in this section has one important drawback. As becomes evident from the last of Eqs. 19, the average rate of active granule cells, a, turns out to be very small, both due to the strong feedback inhibition and the small variance of the excitatory field in Eq. 17. This implies that the signal term in Eq. 11 is also very weak. It means that the network's performance is not robust to any additional sources of noise which are not taken into account in the model, but are necessarily present in real neural systems. This motivated us to turn to another, more complicated model, where all of the interactions

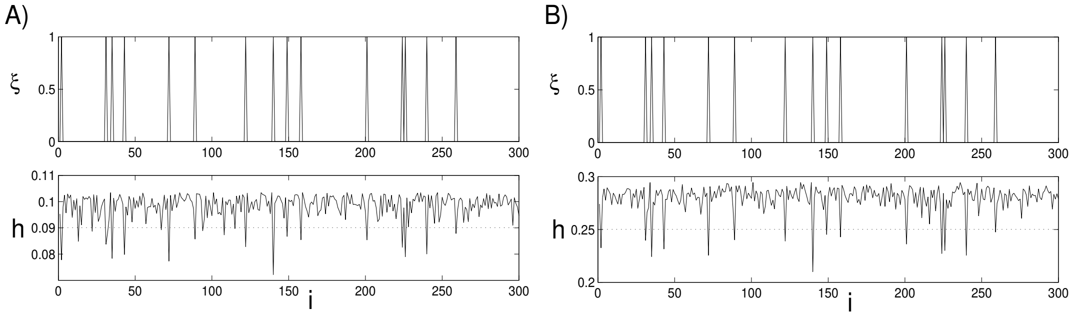

Figure 3: Neuronal activities for Model I with two different choices of N_g/N_m. Both networks were trained on $p = 70$ memory patterns.
A. The input (mitral activity pattern) in a model with $N_m = N_g = 300$, is displayed in the upper box. Below it we present $-h_i$ and I_0 (the dotted line), the inputs to Eq. 3, as a function of the mitral neuron number i. For the pattern to be a consistent memory, these two lines should cross at the same i values for which inputs exist in the upper box. The spurious crossings means that this input cannot be encoded as a memory, hence this is an overloaded network.
B. The same pattern is used as an input to an $N_m = 300$ $N_g = 900$ network, in which case a consistent fixed point is obtained.

in the network are modified during the learning phase.

5 Model II: Learned Connections.

In our second model we allow for Hebbian and inhibitory-Hebbian learning in all three synaptic connection matrices. They are adjusted according to the following learning rules:

$$\begin{aligned} \delta J_{ij} &= \frac{\epsilon}{N_g}(1 - M_i)G_j \\ \delta K_{ij} &= \frac{\kappa}{N_g}\left((1 - G_i)G_j + G_i(1 - G_j)\right) \\ \delta W_{ij} &= \frac{\rho}{N_m} G_i M_j \end{aligned} \tag{20}$$

The motivation for these learning rules is as follows. The first equation leads to an inhibitory-Hebbian structure of the type of equation (6). The second equation replaces the uniform inhibition of the previous model. Its role is to induce competition between the inhibitory cells activated by different patterns, thus preventing the same inhibitory neurons from representing many memories. The third equation introduces a Hebbian modification of the excitatory mitral-granule interactions. It serves to increase the rate of granule cells which are successfully activated by the current pattern. As a result, we expect that even as the fraction of the active granule cells q becomes small, their activity remains finite, i.e. the distribution of the activity in the granule layer becomes bimodal, causing the network to be more robust to external noise.

The Hebbian W_{ij} synaptic connections are excitatory and may be related to the existence of NMDA receptors on granule dendrites. Granule cells were also shown to receive GABAergic (inhibitory) synaptic input whose source is probably neighbouring granule cells(29). This would then correspond to the K_{ij} which facilitate a *disinhibition* mechanism that helps in the construction of Hebbian cell assemblies.

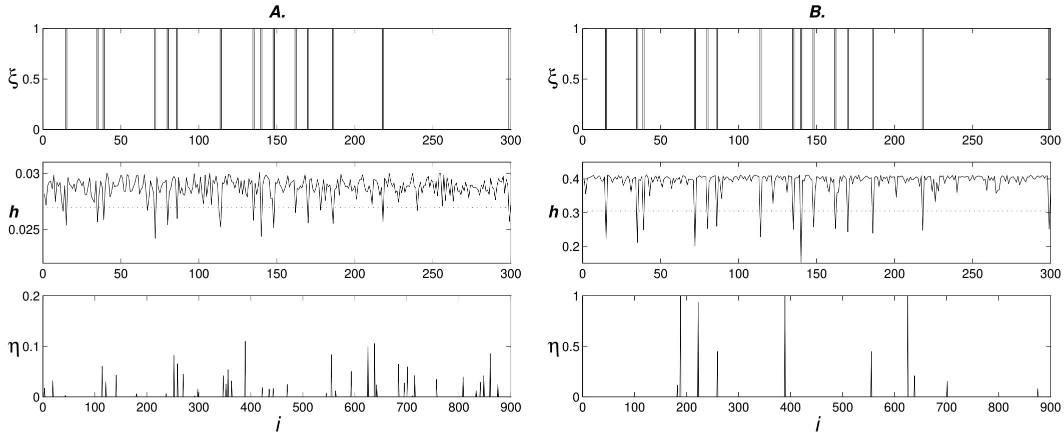

Figure 4: Comparison of Model I with Model II for $N_m = 300$ $N_g = 900$.

A. Model I shows inconsistency between input and output in the case of one of $p = 150$ patterns. We use the same display type as in Fig. 3 for the two upper frames. The lowest frame displays the activity of the granular cells as function of the neuron number. Note the poor signal to noise ratio of the mitral cells.
B. Model II shows a consistent solution and good signal to noise ratio. Note that the scales are different from A. In particular, the granule cells have much higher activities. (Parameters are $\epsilon = 1$ $\kappa = 1$, $\rho = 1$, $\tau_m = 2\tau_g$, $\beta\tau_g = 1$, $dt = \frac{1}{10}\tau_g$)

This model is harder to analyze analytically than the previous one, since the distribution of activities in the granule cells cannot be computed. We perform numerical simulations of the model in order to test its performance. Starting from a network of $N_g = 3N_m$ neurons, we compare an overloaded network of Model I with Model II containing the same number of patterns. Memorization of patterns is carried out iteratively by presenting a set of $p = 150$ patterns over and over again. Figure 4 displays the comparison between the two models. Both contain 300 mitral cells and 900 granule cells. It is clearly visible that the dynamical learning process increases the signal to noise ratio, thus allowing for the bigger capacity of Model II.

It is quite evident from Fig. 4 that the activities of the granule cells are very different in the two models. To understand this difference we display in Fig. 5 a histogram of granule cell activities in both models. This substantiates the claims made before. In Model I there is a peak at zero with a tail which dies out quickly, i.e. the average activation value a is low. In Model II we observe a quite flat distribution, with high values of some individual η_i, leading to a high average a. This is responsible for the better functioning of this model. The learning process chooses individual granule cells to encode the learned memories, thus making efficient use of the synaptic connections which are at its disposal.

6 Discussion

Modeling of the olfactory system has been discussed by many authors. The bulb is generally considered to be a system of odor coding and discrimination (20). The importance of the oscillatory behavior of this system, and, in particular, the fact that it is on the edge of chaos, was emphasized in various publications by Freeman and collaborators(25)(31). A different coding structure within an oscillatory neural network was studied by Li and Hopfield(17). The possibility that this system can serve also the purpose of odor separation was studied by Fort and Rospars(5), Hopfield(14) and Hendin *et al.* (10).

The problematics of modeling the OB as an associative memory was stated in the Introduction. Yao and Freeman(31), as well as Erdi *et al.* (3), try to present realistic modeling of the bulb, yet assume excitatory axodendritic interactions in order to accommodate associative memories. Li and Hopfield(17) don't construct an ordinary associative memory model, but view the odor information as represented by the type of oscillatory motion associated with

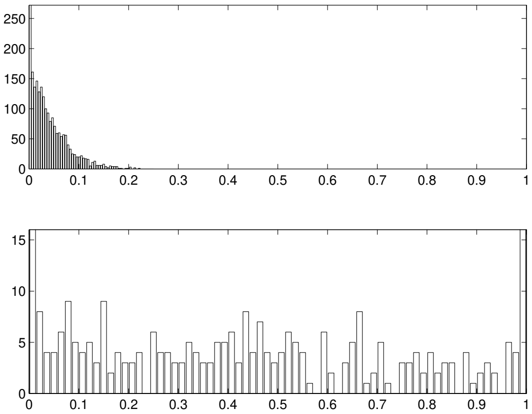

Figure 5: Histogram of the activity distribution in the granule cell layer.

Upper box: Random connectivity between granule cells gives rise to an exponential distribution of low activity.
Lower box: The learning process leads to strong granule activity, distributed along the [0,1] interval, with a pronounced peak at 1.

it.

We propose a model that is an associative memory neural network in the conventional sense, in spite of the fact that we try to adhere to the correct architecture of the bulb. This means that we don't assume any lateral excitatory-excitatory connections, and we have many more granule than mitral cells. Furthermore, we construct a model based on dendrodendritic interactions only. At the present stage our model is dissipative and moves into fixed points. We have convinced ourselves that it will perform well also under oscillatory conditions, and will demonstrate this elsewhere, incorporating the present associative neural network of the external plexiform layer in a more detailed model of the bulb.(11)

To construct an ANN we needed a new source for the nonlinearity, and we chose the rate of neurotransmitter release for this purpose. We have shown that associative memory can be implemented in this system. We verified that the capacity for patterns $\{\xi\}$ which are defined with respect to the activity of N_m mitral cells, depends on the number of granule cells N_g. As $N_g \to \infty$ we find that for finite activity q the capacity p_{max} is constant, and for $q < N_g^{-1/3}$ it scales with $\sqrt{N_g/q}$. However low this limit seems, we should examine its agreement with our knowledge of the real biological network we are modeling. When using high activity values such that the theoretical limit is $p_{max} = 1/fq^2$ we see that $f = q = 0.05$ gives $p_{max} = 8,000$. This number of memorized odors is probably much larger than an animal has to remember in its lifetime. In addition, 5% active neurons during recall corresponds to activity levels that are much higher than those observed in the bulb of living rabbits during exposure to familiar odors, or that can be inferred from 2DG experiments performed on rats (24) (23). Hence, we conclude that many more patterns of lower activity levels can be stored in this naive and seemingly low capacity network.

The olfactory cortex receives information on external odor stimuli via the projections of excitatory mitral cells. For this reason we identify odor memories with activity patterns of mitral cells. Yet, the analysis of our model reveals, that the maximal number of memories which can be stored in the network grows with the size of the inhibitory population. A similar conclusion was reached by Frolov & Muraviev (6) from an information-theoretical point of view. This provides a possible theoretical understanding for the abundance of granule cells in the olfactory bulb(21).

As already stated before, we chose to concentrate here on an ANN with convergence dynamics, i.e., upon presentation of a memory pattern, the neural activity flows into a fixed point. One can accommodate oscillatory behavior in our system by appropriate choices of the strength of the excitatory and inhibitory interactions (e.g., replacing $\kappa = 1$ in the retrieval mode of Model II by 0.1 leads to oscillatory retrieval). We preferred to work in a parameter regime in which the dynamic attractors were only fixed points, in order to be able to perform analytic and numerical estimates of the capacity. We have evidence that oscillatory behavior does not change our conclusion that the EP layer of the OB can serve as an ANN.(11)

Finally we wish to draw attention to the major ingredients of Model II, the connections between granule and mitral cells. These synapses are modified in an activity-dependent manner during the learning phase. We argue that an appropriate learning rule for these connections is an 'inhibitory-Hebb' one, implying reinforcement of the synaptic connection between an active inhibitory neuron and a quiescent excitatory postsynaptic cell. We have shown that the improved performance in Model II is due to this learning rule. In this model the system makes good use of the inhibitory neurons in order to encode memory patterns. The inhibitory neurons are assigned an important informative role, thus serving as major players in the encoding task, rather than being only agents for competition between excitatory neurons as in many conventional neural models.

Appendix

Here we outline the solution of Model (I) leading to Eqs. 19. Given that the input to granule cells is a sum of the gaussian random excitation h_i^{ex} and uniform inhibition $-\kappa\langle G\rangle$. We take into account Eq. 5, choosing $\beta\tau_g = 1$, and obtain the following distribution of activity in the granule cell layer G_i:

$$Prob(G) = \begin{cases} Prob(h^{ex} < \kappa\langle G\rangle) & \text{for } G = 0 \\ Prob(h^{ex} = G + \kappa\langle G\rangle) & \text{for } G > 0 \end{cases} \tag{21}$$

The average activity of the granule cells can be found from the self – consistency condition:

$$\langle G\rangle = \sum_G G Prob(G) \tag{22}$$

With h^{ex} being of gaussian distribution, this becomes:

$$\langle G\rangle = v\Phi_1\left(\frac{\kappa\langle G\rangle - \langle h^{ex}\rangle}{v}\right) \tag{23}$$

Where Φ_1 is one of a family of functions, related to the gaussian distribution:

$$\Phi_n(x) = \frac{1}{\sqrt{2\pi}}\int_x^{\infty}(t-x)^n \exp\left(-\frac{t^2}{2}\right)dt \qquad \text{for} \qquad n = 0, 1, 2, \cdots \tag{24}$$

Similarly, the fraction of the active granule cells can be obtained by:

$$q = \Phi_0\left(\frac{\kappa\langle G\rangle - \langle h^{ex}\rangle}{v}\right) \tag{25}$$

We are interested in the asymptotic solution of the Eqs. 23, 25 in the limit of strong inhibition, when most of the granule cells are silent, i.e. $\kappa\langle G\rangle - \langle h^{ex}\rangle \gg v$. One can use the asymptotic expressions of the functions

$$\Phi_n(x) \approx \frac{n!}{(2\sqrt{\pi})x^{n+1}} \exp\left(-\frac{x^2}{2}\right) \tag{26}$$

for solving Eqs. 23, 25, resulting in Eqs. 19.

Acknowledgments

O.H. thanks Prof. Idan Segev for very fruitful discussions.

References

[1] Agmon-Snir H., and Segev I. (1993) Signal Delay and Input Synchronization in Passive Dendritic Structures. J. of Neurophysiol. Vol. 70, No. 5, pp. 2066-2085.

[2] Davis J. L. and Eichenbaum H. (eds) (1991) Olfaction. MIT press.

[3] Erdi P., Grobler T., Barna G., Kaski K. (1993). Dynamics of the olfactory bulb: bifurcations, learning, and memory. Biol. Cybern. vol. 69, pp. 57-66.

[4] Farbman A. L. (1991) Development neurobiology of the olfactory system. In *Smell and Taste in Health and Disease.* Getchel T.V. Doty R.L. Batoshuk L.M. Snow J.B. (Editors) New York: Raven Press pp. 19-33.

[5] Fort J. C. and Rospars J. P, 1992. Modelling of the qualitative discrimination of odours in the first two layers of olfactory system by Jutten and Herault algorithm. Comptes Rendus de L Academie des Sciences. Serie III, Sciences de la Vie, 315(9):331-6.

[6] Frolov A. and Muraviev I. (1988) Informational characteristics of neural networks. Moscow, Nauka. (In Russian).

[7] Gardner E. (1987) Maximum Storage Capacity in Neural Networks. Europhys. Lett., 4 (4), pp. 481-485.

[8] Hasselmo M. E. (1993) Acetylcholine and Learning in a Cortical Associative Memory. Neural Computation Vol. 5, No. 1.

[9] Hasselmo M. E. and Bower J. M.(1993) Acetylcholine and memory. Trends in Neurosciences, 16(6) pp. 218-22.

[10] Hendin O., Horn D. and Hopfield J. J. (1994) Decomposition of a Mixture of Signals in a Model of the Olfactory Bulb. Proc. Natl. Acad. Sci. Vol. 91 No. 13 pp. 5942-5946.

[11] Hendin O., Horn D. and Tsodyks, M. V. Associative Memory and Segmentation in an Oscillatory Neural Model of the Olfactory Bulb. Preprint.

[12] Hopfield J. J. (1982) Neural networks and physical systems with emergent collective computational abilities. Proc. Natl. Acad. Sci. USA 79, pp. 2554-2558.

[13] Hopfield J. J. (1984) Neurons with graded response have collective computational properties like those of two-state neurons. Proc. Natl. Acad. Sci. USA 81, pp. 3088-3092.

[14] Hopfield J. J. (1991) Olfactory computation and object perception. Proc. Natl. Acad. Sci. USA, pp. 6462-6466.

[15] Jahr C. E. and Nicoll R. A. (1982). An intracellular analysis of dendrodendritic inhibition in the turtle in vitro olfactory bulb. J. Physiol. (lond.) 326: pp. 213-234.

[16] Laurent G. and Davidowitz H. (1994) Encoding of olfactory information with oscillating neural assemblies. Science, vol. 265, pp. 1872-1875.

[17] Li Z. and Hopfield J. J. (1989). Modeling the Olfactory Bulb and its Neural Oscillatory Processings. Biol. Cybern. vol. 61, pp. 379-392.

[18] Luskin M. B. (1993) Restricted proliferation and migration of post natally generated neurons derived from the forebrain subventricular zone. Neuron 11, pp. 173-189.

[19] Ressler K. J., Sullivan S.L. and Buck L.B. Information Coding in the Olfactory System: Evidence for a Sterotyped and Highly Organized Epitope Map in the Olfactory Bulb. Cell vol. 79, pp. 1245-1255.

[20] Schild D. (1988). Principles of Odor Coding and a Neural Network fo odor discrimination. Biophys. J. Vol. 54, pp. 1001-1011.

[21] Shepherd G. M. (1979). The Synaptic Organization of the Brain, Oxford Univ. Press, New York.

[22] Shepherd G. M. (1992). Modules for molecules. Nature 358, pp. 457-458.

[23] Stewart W. B., Kauer J. S. and Shepherd G. M. (1979) Functional organization in rat olfactory bulb analysed by the 2-deoxyglucose method. J Comp. Neurol. 185, pp. 715-734.

[24] Sharp F. R., Kauer J. S. and Shepherd G. M. (1975) Local sites of activity related glucose metabolism in rat olfactory bulb during olfactory stimulation. Brain Res. 98. pp.596-600.

[25] Skarda C. A. and Freeman W. J. (1987) How brains make chaos in order to make sense of the world. Behavioral and Brain Sci. 10, pp. 161-195.

[26] Tsodyks M. V. and Feigelman M. V. (1988) The Enhanced Storage Capacity in Neural Networks with Low Activity Level. Europhys. Lett., 6 (2), pp. 101-105.

[27] Vassar R., Chao S.K., Sitcheran R., Nunez J. M., Vosshall L. B. and Axel R. (1994) Topographic Organization of Sensory Projections to the Olfactory Bulb. Cell, Vol. 79, pp. 981-991.

[28] Wellis D. P. and Scott J. W. (1990) Intracellular Response of Identified Rat Olfactory Bulb Interneurons to Electrical and Odor Stimulation J. of Neurophysiology, Vol. 64, No. 3, pp. 932-947.

[29] Wellis D. P. and Kauer J. S. (1994) GABAergic and glutamatergic synaptic input to identified granule cells in salamander olfactory bulb. J. of Physiology, Vol. 475.2, pp. 419-430.

[30] Willshaw D., Buneman O. P. and Longuet-Higgins H. (1969) Non-Holographic Associative Memory. Nature Vol 222 pp. 960-962.

[31] Yao Y. and Freeman W. J. (1990). Model of biological pattern recognition with spatially chaotic dynamics. Neural Networks, 3, pp. 153-170.